SSIM 2023 – PM Dight (ed.)

doi:10.36487/ACG_repo/2335_02

# Integrated hydrogeological and geotechnical studies at the Diavik Diamond Mine in support of pit slope design optimisation

**J Levenick** *WSP, Canada*

**D Chorley** *WSP, Canada*

**C Dourado** *WSP, Canada*

**K Jain** *WSP, Canada*

**M Valerio** *WSP, Canada*

**S Ross** *WSP, Canada*

**M Chivasa** *Rio Tinto, Canada*

## Abstract

*Integrated hydrogeological and geotechnical studies have been critical for slope stability analysis and pit slope design at the Diavik Diamond Mine A21 pit in the Northwest Territories of Canada, an area of continuous permafrost. The mine is located on the shores of Lac de Gras and required partial dewatering of a lake with the associated construction of a water-retention dyke to facilitate the pit excavation within the underlying open talik (unfrozen ground).*

*Pre-feasibility hydrogeological modelling of the pit identified the need for a dewatering well network to achieve the design acceptance criteria for the pit walls. Testing of initial dewatering wells installed along the pit crest identified the potential presence of an unmapped structural feature/enhanced permeability zone behind the southeast wall of the pit. This triggered further detailed review of core logs and available mapping data, which corroborated the presence of a highly fractured zone for consideration in both the hydrogeological and slope stability modelling in support of detailed pit slope design and optimisation.*

*Over the course of the mine life, multiple revisions of the hydrogeological model have been made as supplemental data has been collected to support refinement of pore pressure predictions behind the pit walls. The groundwater modelling considered the inherent uncertainty of modelling in bedrock environments and the efficiency of pumping wells in fractured bedrock, and was completed in close collaboration with geotechnical teams to successfully support slope stability analysis and design optimisation.*

**Keywords***: dewatering, groundwater model, slope stability, well efficiency*

## 1 Introduction

The Diavik Diamond Mine is situated in an area of continuous permafrost 300 km northeast of Yellowknife, with permafrost extending to depths of up to 400 m below land and below large lake islands. Permafrost is virtually impermeable, isolating the deep groundwater flow regime beneath the permafrost from infiltrating precipitation. Consequently, the regional groundwater flow below the deep permafrost is generally controlled by the water levels in lakes within taliks (unfrozen ground) that extend below large lakes.

The A21 pit at Diavik is located on the shores of Lac de Gras, an extensive freshwater lake (Figure 1). Open pit mining of the A21 kimberlite pipe required partial dewatering of the lake and the associated construction of a water-retention dyke to facilitate pit excavation within the underlying open talik. The steep slopes of the A21 pit, combined with the water-retention dyke setback, led to the pit slope stability being sensitive to

water pressures and the requirement for a pit depressurisation system to meet the design acceptance Factor of Safety (FoS) criteria.

Design of the pit depressurisation system and prediction of pore pressures behind the pit slopes were undertaken using a numerical groundwater model. Over the course of the mine life, multiple revisions of the hydrogeological model have been made as supplemental data has been collected to support refinement of pore pressure predictions behind the pit walls and evaluation of the performance of the dewatering systems. This paper presents four aspects of the project that led to the successful evaluation of pore pressures behind the pit walls over the life of mine:

- The data review that led to the identification of an enhanced permeability zone (EPZ).
- The approach adopted in model calibration in consideration of the uncertainty of simulating bedrock environments.
- The approach adopted in the modelling to incorporate observed well efficiency into the prediction of future hydraulic heads.
- The use of an observational mining method and pore pressure reconciliation in the final stages of mining.

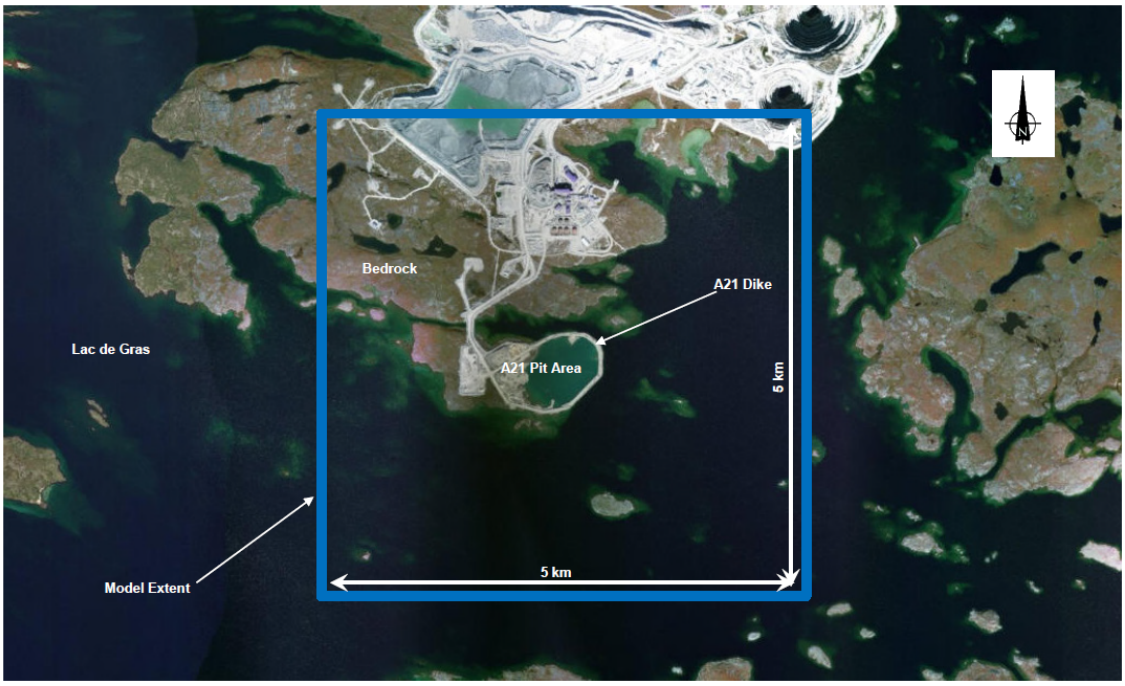


**Figure 1 A21 pit area and groundwater model domain extent**

# 2 Background

## 2.1 Regional geology and structures

Lac de Gras is in the central part of the Slave geological region in the Canadian Shield, the largest physiographic region in Canada. The main surficial deposits in the project area consist of lakebed sediments and glacial till. The surficial deposits are underlain by granite and pegmatite country rocks that intrude metasedimentary rocks originally deposited as sandstones and shales. The granitoid and metasedimentary country rocks are Late Archean in age (2.5 to 2.8 billion years old) and belong to the cratonic Slave Structural Province. The metasedimentary units generally represent only a small proportion of the country rock, occurring as metasedimentary rafts within the intrusive complex. Diabase dyke swarms of Proterozoic age

(1.3 to 2.2 billion years old) intrude the granitoid and metasedimentary rocks. The kimberlite pipes are Eocene in age (54 to 58 million years old) and intrude both the Archean and Proterozoic units.

The A21 pit area is underlain by tonalite to quartz diorite, described as medium grained with biotite and hornblende to 35%. In some cases, the units may be foliated or lineated. Locally, quartz and/or biotite concentration is reduced, and the bulk composition is of leucogabbro, gabbro or diorite, which is typically coarse grained with pockmarked weathered surfaces. Pegmatite dykes intrude the tonalite, and consist of microcline and quartz, muscovite, and locally abundant biotite, tourmaline and garnet. The dykes are considered to be comagmatic with the pegmatitic 2-mica granite.

The tonalite is intruded by kimberlite pipes, with the A21 kimberlite pipe consisting of weak volcaniclastic kimberlite and kimberlitic mudstone with occasional hypabyssal kimberlite intrusions, especially along the pipe margins. The kimberlite pipes at Diavik tend to be aligned along a northeast-trending axis representing a zone of structural weakness that the intrusions have exploited. At the A21 pit, Joe's Fault is a significant structural zone identified along a northeast-southwest trend and consists of two parallel faults approximately 50 m apart that are associated with a bathymetric low extending from the A21 pipe to the southwest (Figure 2).

A bathymetric depression referred to as 'Deep Blue' was identified as part of surveys done prior to lake dewatering to the southwest of the A21 kimberlite pipe. This permeable feature is characterised by increased rock alteration, fracturing and faults dipping at shallow to moderately steep angles. The rock types of the Deep Blue feature below the bathymetric depression are tonalite and pegmatite to the depths investigated by drilling and exposed during mining.

After mining commenced, a third significant permeable feature was identified in the southeast wall during the installation of the pit depressurisation system. This feature is interpreted to be structurally controlled and bound by Joe's Fault to the west and by a less permeable structure (Stubley 2 Fault) to the south (Figure 3).

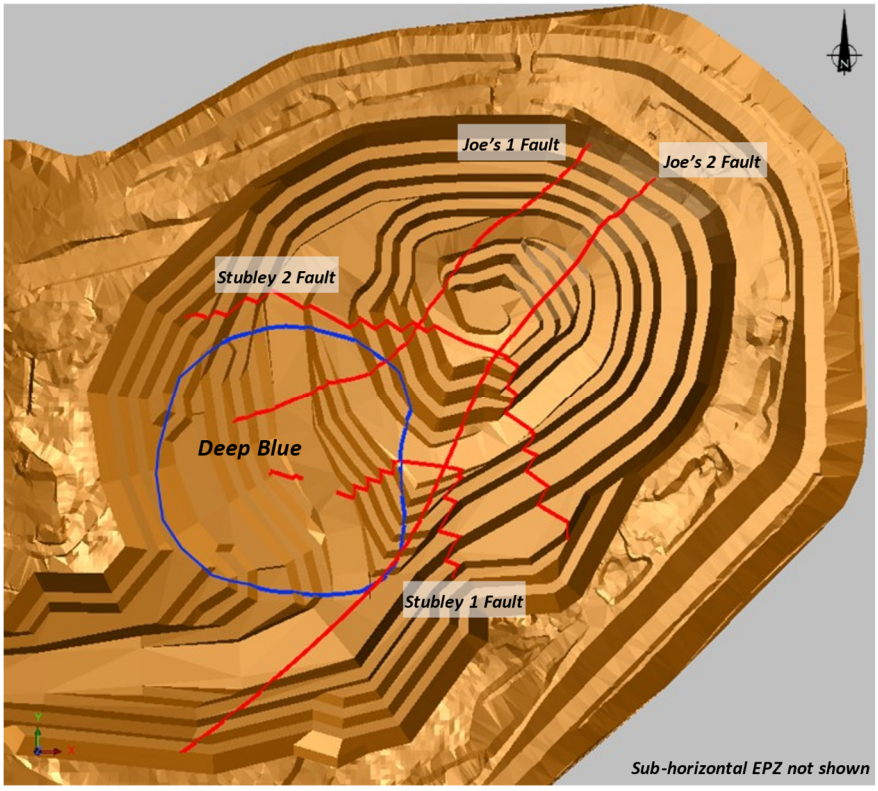


**Figure 2 Location of enhanced permeability zones at A21 pit – plan view**

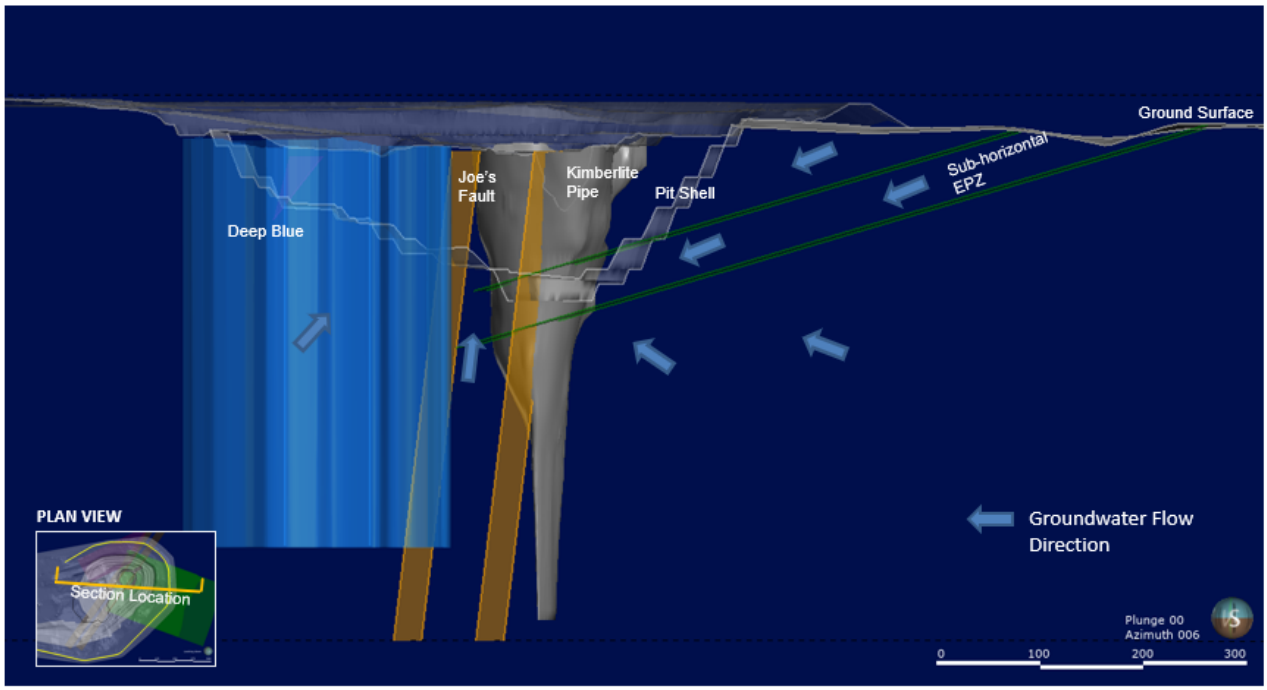


**Figure 3 Location of A21 sub-horizontal enhanced permeability zones – cross-section view**

## 2.2 History of groundwater modelling

Regional numerical hydrogeologic models were developed in MODFLOW for the Diavik mines, including A21, in the mid- to late-1990s for feasibility and environmental assessment purposes. The A21 model was subsequently updated in 2006 and 2012 to incorporate additional hydrogeological information obtained during field investigations at the A21 pipe and the model code was converted from MODFLOW to FEFLOW. In the 2012 update, the geotechnical and hydrogeological feasibility assessment identified that effective slope depressurisation would be a critical component of slope stability management. The pit slope stability analysis for the ultimate pit suggested that depressurisation would be required in the northwest, northeast and southeast sections of the pit to meet FoS design acceptance criteria (DAC). Mitigation scenarios, where depressurisation wells would be drilled from the crest and 350 masl bench (9,350 mine grid elevation), were iteratively simulated using the developed groundwater model until a final depressurisation system was identified that was predicted to meet FoS DAC. The model predicted that the pit depressurisation system was not needed at the start of mining but would be required once the pit depth reached 350 masl.

In 2018, the pit depressurisation system began a phased installation. The first phase of the A21 depressurisation program consisted of the advancement of 11 steeply dipping pumping wells towards the pit. The wells were installed along the crest of the southeast wall (nine locations) within the northeast-trending Joe's Faults (at one location, A21-DP-12 [well 19]) and in the flooded underground exploration decline near the pit (at one location, A21-DP11 [well 41 ]). Concurrent with this program, 11 piezometer boreholes, each consisting of five grouted-in vibrating wire transducers, were installed near these wells to monitor the pressure response to pumping of the depressurisation wells. Over subsequent years, the pit depressurisation system was expanded to include 21 wells along the pit crest and six wells (DBW series) in the Deep Blue permeable feature, with a network of 84 vibrating wire piezometers (VWP). The location of the depressurisation wells and piezometers are shown in Figure 4. The model was calibrated in 2018 following the installation of the first phase of the A21 depressurisation system and recalibrated in 2021 following a revision of the structural model and a significant expansion of the A21 depressurisation system into Deep Blue, which provided an enhanced calibration dataset under higher pumping stresses.

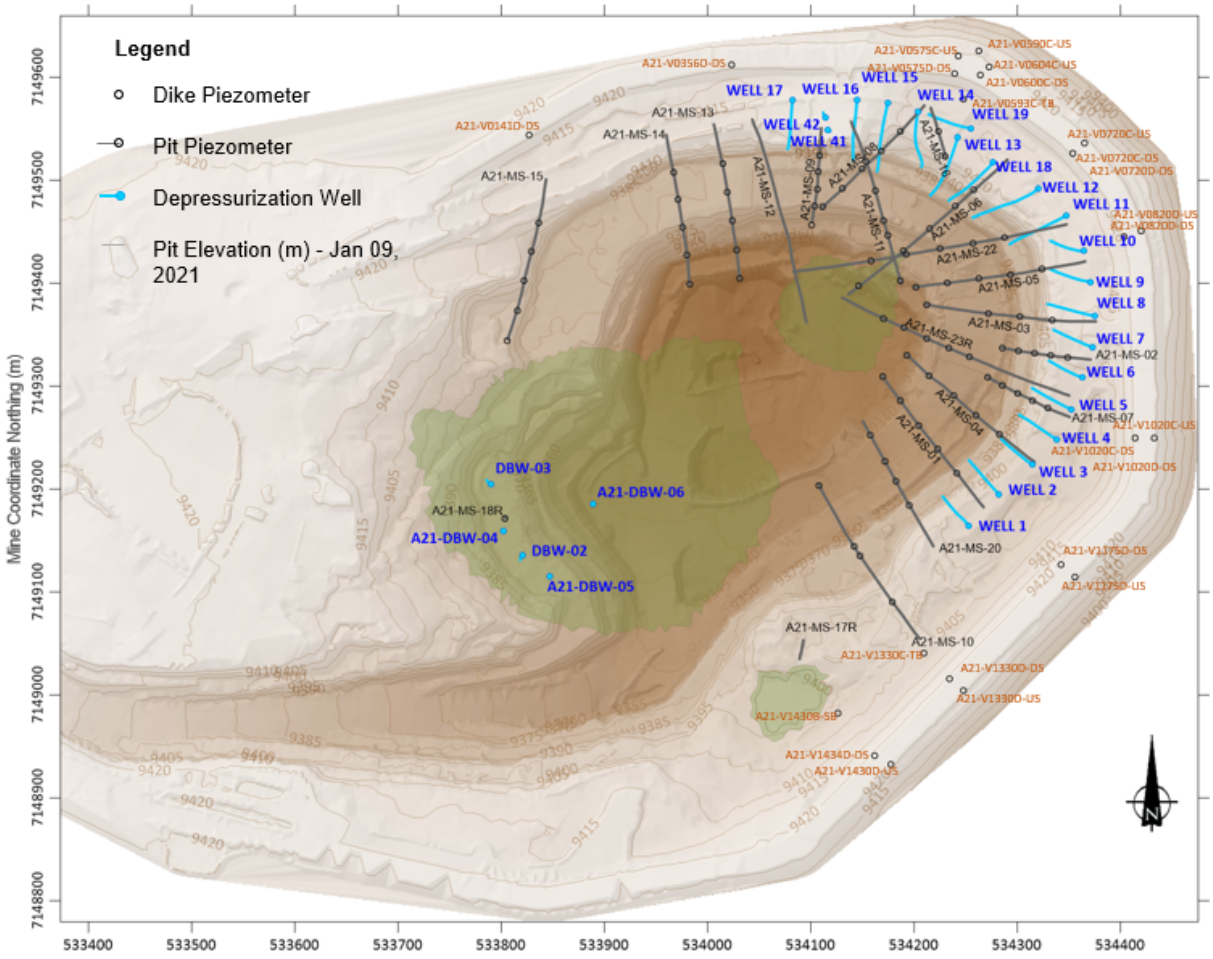


**Figure 4 Location of A21 depressurisation wells and vibrating wire piezometers**

## 2.3 Conceptual hydrogeological model

A conceptual hydrogeological model is a representation of the groundwater regime that organises and simplifies the site hydrogeology so that it can be modelled more readily. This conceptual model must retain sufficient complexity for the numerical model developed from it to adequately reproduce or simulate to the degree required to meet the project objectives: the real groundwater behaviour. Based on an interpretation of the available data, the following presents the conceptual model of the groundwater regime at the site.

In consideration of the regional setting, the conceptual model incorporated in the numerical groundwater model consisted of the following hydrostratigraphic units:

- Surficial deposits (till) ($10^{-6}$ m/s).
- Weathered bedrock ($10^{-6}$ m/s).
- Competent bedrock (including tonalite, pegmatite, and minor diabase dykes and metasediments) ($10^{-6}$ to $10^{-9}$ m/s, decreasing with depth).
- Kimberlite ($10^{-7}$ m/s) and a thin contact zone around the kimberlite ($10^{-6}$ to $10^{-7}$ m/s, decreasing with depth).
- Joe's Fault ($10^{-6}$ to $10^{-8}$ m/s, decreasing with depth).
- Stubley Fault 1 and 2 ($10^{-5}$ to $10^{-9}$ m/s, decreasing with depth).
- A21 sub-horizontal EPZ ($10^{-6}$ m/s).

- An EPZ associated with the Deep Blue bathymetric depression ($10^{-5}$ to $10^{-6}$ m/s, decreasing with depth).

Prior to mining the A21 kimberlite pipe, static water level measurements indicated that groundwater beneath Lac de Gras was under near-hydrostatic conditions. This is consistent with the presence of the lake acting as an extensive constant head boundary and the isolation of the deep regional groundwater flow system from recharge above the permafrost on the islands and mainland. During mining, the open pit is a sink for groundwater flow. The presence of the lake behind the water-retention dyke acts as a strong constant head boundary to groundwater flow. Seepage faces will be present on the pit walls. Water will be induced to flow from the lake through the lakebed sediments, beneath the low permeable core of the water-retention dyke and through the bedrock into the open pit. Bedrock between the water-retention dyke and the pit crests will be partially desaturated, and the watertable will slope steeply from the base of the water-retention dyke core to the open pit. The presence of EPZ, including Deep Blue and other permeable structures, will act as drains, and the watertable in these zones may be lower than in areas of tight rock.

# 3 Identification of an enhanced permeability zone

As described previously, the first phase of the A21 depressurisation program was completed in 2018 and consisted of the installation of 11 wells and a network of VWP to monitor pressure response to pumping of the depressurisation wells (Figure 5). Pumping tests were carried out in the depressurisation wells between June and August 2018 as the individual wells were being completed. During each pumping test, pore pressure responses were monitored and recorded in the piezometers. The pumping rate for the well installed in the Joe's Faults was 6.2 L/s and the pumping rates for the wells on the southeast and northeast walls, where pumping could be sustained, varied from 0.6 to 2.8 L/s, with higher pumping rates generally associated with proximity to Joe's Faults. Only limited information was collected from the well A21-DP-12 (well 41) installed within the flooded underground decline because it could only be pumped for 2.5 hours.

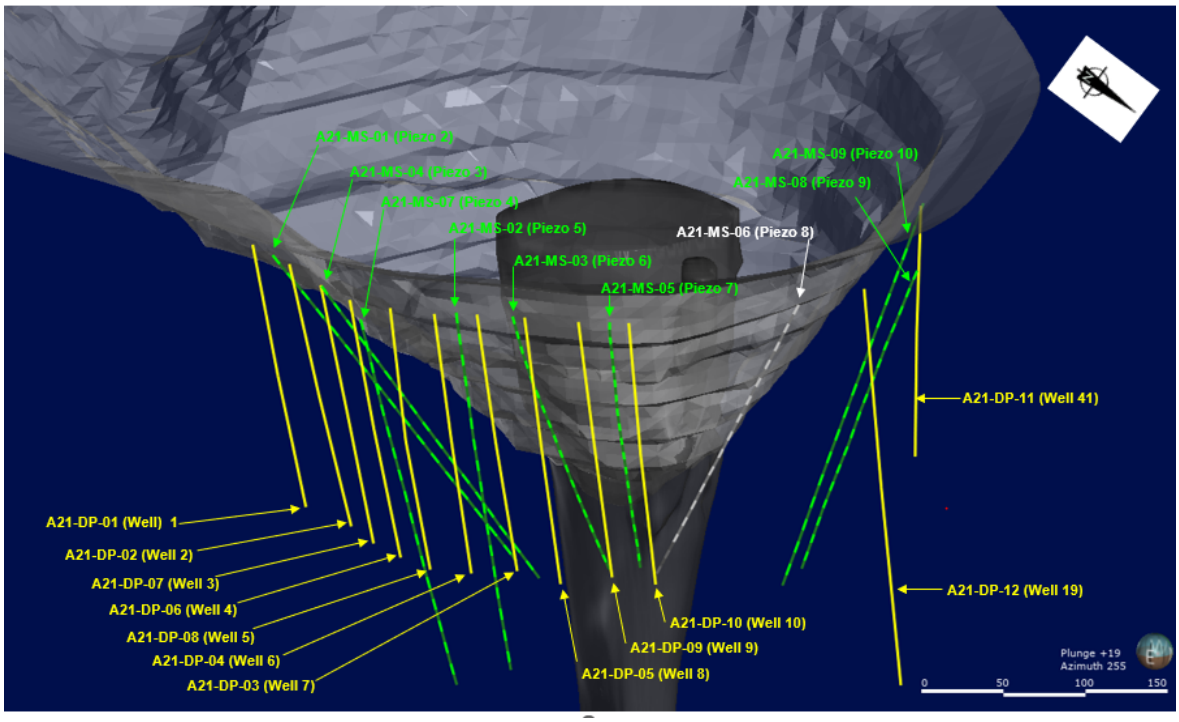


**Figure 5 Location of the 2018 depressurisation wells and pit vibrating wire piezometers**

Review of data collected during the individual pumping tests and during the commissioning of the Phase 1 depressurisation system identified a zone of higher drawdowns at depth in piezometers installed in the southeast wall, with lower magnitude drawdowns observed both above and below this interval (Figure 6).

The zone of higher drawdown corresponds reasonably well with airlifting observations during drilling. During airlifting, higher flows were observed below 250 to 300 masl (9,250 to 9,300 m mine grid elevation) (Figure 7).

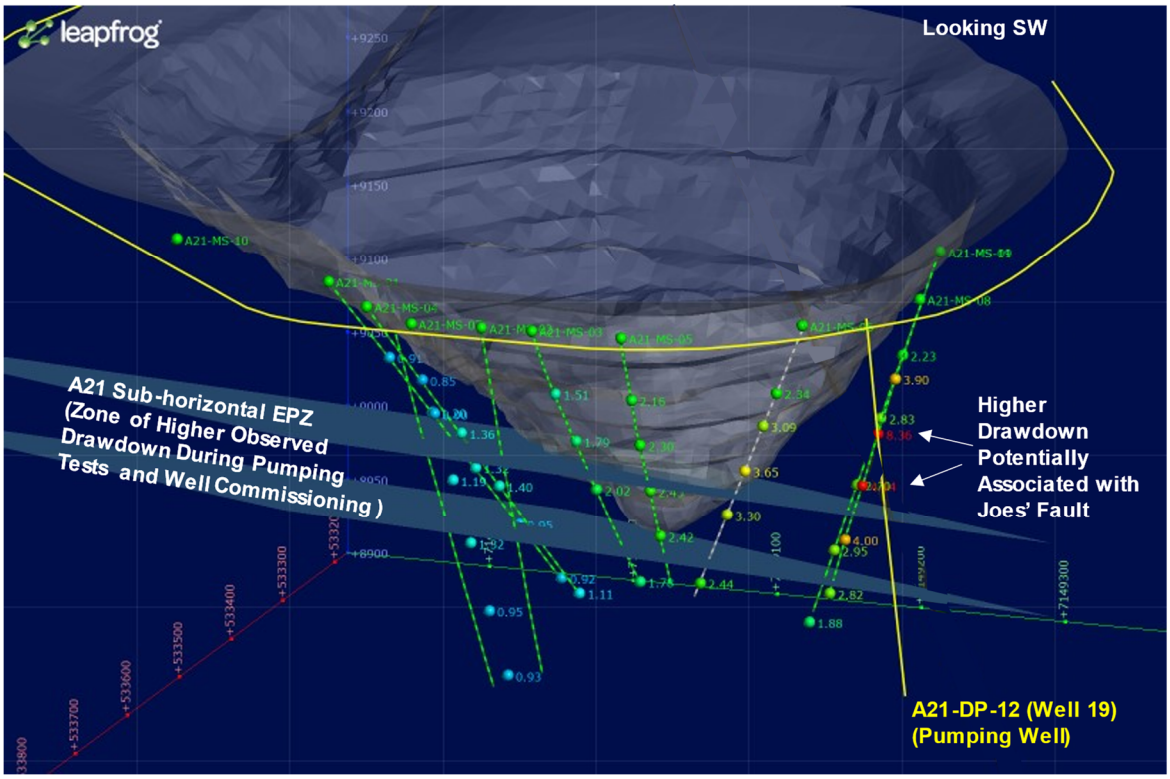


**Figure 6 Observed drawdown A21-DP-12 (well 19) pumping test**

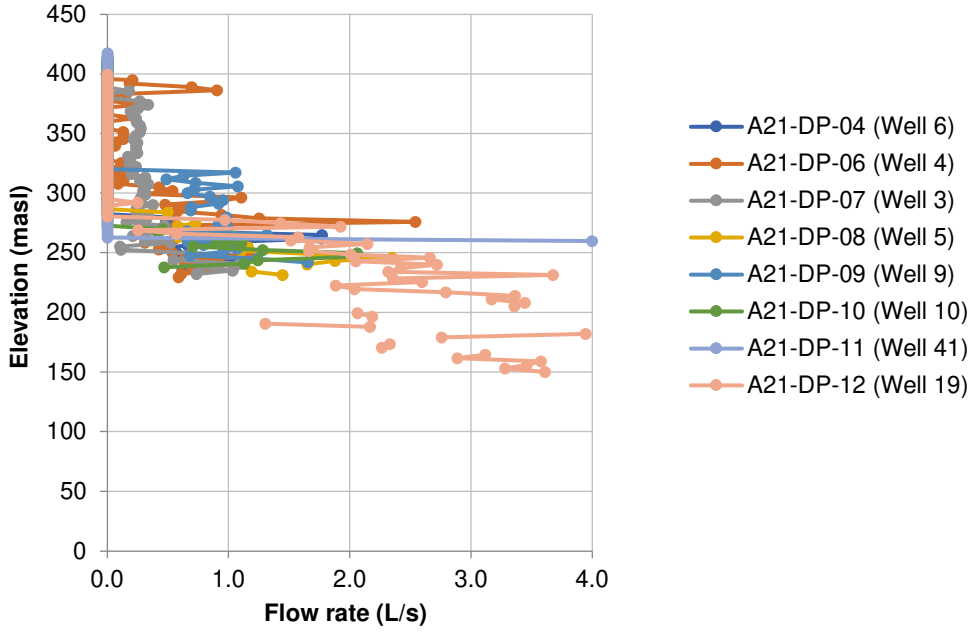


**Figure 7 Observed flow rates during airlifting tests**

Figure 6 presents the zone of increased drawdown, as evidenced by the observed drawdown in hydraulic head across the piezometer network during the A21-DP-12 (well 19) pumping test. Review of the of the geotechnical data after identification of this zone found that the orientation was consistent with a sub-horizontal joint set orientation identified during the geotechnical feasibility study. It was also generally consistent with observed open structures (>20 mm). Based on the pumping test analysis, and the

confirmation with geotechnical data, an EPZ was inferred to be present over a 50 m interval in the southeast wall. It was postulated that the increased hydraulic conductivity was likely associated with increased joint aperture and/or increased connectiveness of the joints or fractures in this area. This EPZ is herein referred to as the A21 sub-horizontal EPZ. The structure was further verified in 2021 when an A21 structural characterisation review was undertaken that included the sub-horizontal EPZ. An analysis of structural data (fracture frequency and orientation) from A21 geotechnical boreholes and photogrammetry mapping data supported the presence of a sub-horizonal EPZ with concentrations of open structures dipping at shallow angles towards the northwest in the east structural domain between elevations of approximately 300 and 250 masl, mainly associated with pegmatite intrusions.

The A21 sub-horizontal EPZ was a significant feature in the southeast wall that influenced pore pressures and dewatering requirements. Its identification indicates the need to critically review all data collected as part of hydrogeological investigations for the presence of unmapped features and to integrate that knowledge with the conceptual models incorporated in the geotechnical and hydrogeological models.

# 4 Approach to model calibration considering the complexity of a fractured bedrock environment

## 4.1 Calibration methodology

During calibration the model was run repeatedly, and the model parameters iteratively adjusted until a reasonable agreement between predicted and measured hydraulic heads and pit inflow rates were obtained. Early calibration efforts in 2018 were completed using transient model simulations. However, as mining progressed, it was identified that the bedrock storage was sufficiently low that there was minimal time lag between changes in pit depressurisation/mine excavation and changes in pore pressures in the VWPs. Calibration was then changed in 2021 to a series of steady-state simulations, with simulations corresponding to major milestones in the pit progression or expansion of the pit depressurisation network. The advantage of the steady-state simulations was the speed of model simulations, which facilitated running a large number of simulations using both automated (FE-Pest software) and manual adjustments. The seven calibration stages considered are:

- Phase 1 – Re-pumping – October 2018.
- Phase 2 – Infield pumping wells operational along pit crest – November 2018.
- Phase 3 – Expanded infield pumping well network operation – December 2019.
- Phase 4 – Pumping wells added in Deep Blue – May 2020.
- Phases 5, 6 and 7 – Increased pumping in Deep Blue – February 2021, April 2021 and August 2021, respectively.

Calibration to piezometer measurements was supplemented by calibration to pit inflows reporting to pit sumps outside of spring freshet and summer precipitation events.

## 4.2 Measured versus predicted hydraulic heads and prediction uncertainty

The model was calibrated to measured inflows to the open pit and to hydraulic head measurements across the piezometer network. For the hydraulic heads, the two primary metrics were the spatial distribution of residuals (difference between measured and predicted hydraulic head), and the normalised root mean squared error (RMSE). RMSE is a statistical measure of the mean difference between the predicted and measured hydraulic head (h), i.e. residual head. The normalised RMSE (NRMSE) is the RMSE divided by the range of observed hydraulic head values and is commonly expressed as a percentage. Generally, NRMSE under 10% is considered acceptable for model calibration, though for fractured bedrock environments such as near A21, where compartmentalisation occurs, this target can be impractical to achieve.

$$RMSE = \sqrt{\frac{1}{n}\sum_{i=1}^{n} h_{predicted} - h_{measured}} \quad (1)$$

$$NRMSE = \frac{RMSE}{max\ h_{measured} - min\ h_{measured}} \quad (2)$$

Bedrock environments are inherently heterogeneous and sensitive to bedrock structure. The NRMSE for the calibration phases ranged from 7 to 39%, which is higher than typically accepted for some model calibrations but considered reasonable and the practical limit for the modelling effort, given the complexity of the fractured bedrock near the A21 pit. Structures are complex and undergoing periodic revision as new data is included/exposed during mining. Compartmentalisation was observed in the bedrock as evidenced by the water level trends in piezometers and in the pumping test analysis associated with the pumping wells, where the well efficiency owing to formation losses (not well construction) was very low at 8%. Variability will also be present from localised variations in bedrock permeability around the wells (heterogeneous jointing/ fractures), which will affect responses to pumping.

Given the complexity and uncertainty in bedrock environments, the model was calibrated to achieve a slight tendency towards overpredicting hydraulic heads, which from a geotechnical stability perspective is conversative as it means the model under-predicts the pore pressure reduction. (Example plots of calibration comparisons of measured versus predicted hydraulic heads and drawdowns are shown in Figures 8 and 9). Spatial residuals (differences between measured and predicted hydraulic heads) were reviewed across the pit to indicate zones of poorer calibration that should be considered in the slope stability modelling uncertainty analysis. The mean error for the calibration phases ranged from less than -1.4 m (Phase 7) to 6.7 m (Phase 6) and, except for the last phase, indicated a slight tendency to overpredict hydraulic heads. Review of spatial residuals (the difference between measured and predicted hydraulic head or drawdown) indicate that the model tends to underestimate hydraulic heads (overpredict drawdown) in the upper benches of the north wall, and a conceptual model could not be identified in the calibration process that would eliminate this bias. From a geotechnical stability perspective this is not conservative and was therefore relayed to the geotechnical team such that it could be considered in the uncertainty analysis for the slope stability work.

# 5 Well efficiency and its consideration in future model predictions

Future predictions of pore pressures in the pit walls require reasonable simulation of the effects of dewatering wells as they are installed. The wells at the A21 open pit during the initial phase of installation were found to be inefficient due to the nature of the bedrock formation, and this inefficiency required consideration in the method of simulation in the groundwater model such that the reduction in pore pressures from future dewatering wells could be evaluated. This was achieved in a two-step process, with an initial estimation of well efficiency from testing of the Phase I installation of the dewatering well network, followed by a modification of the boundary conditions in the model representing supplemental dewatering wells according to the estimated well efficiency of the already installed wells.

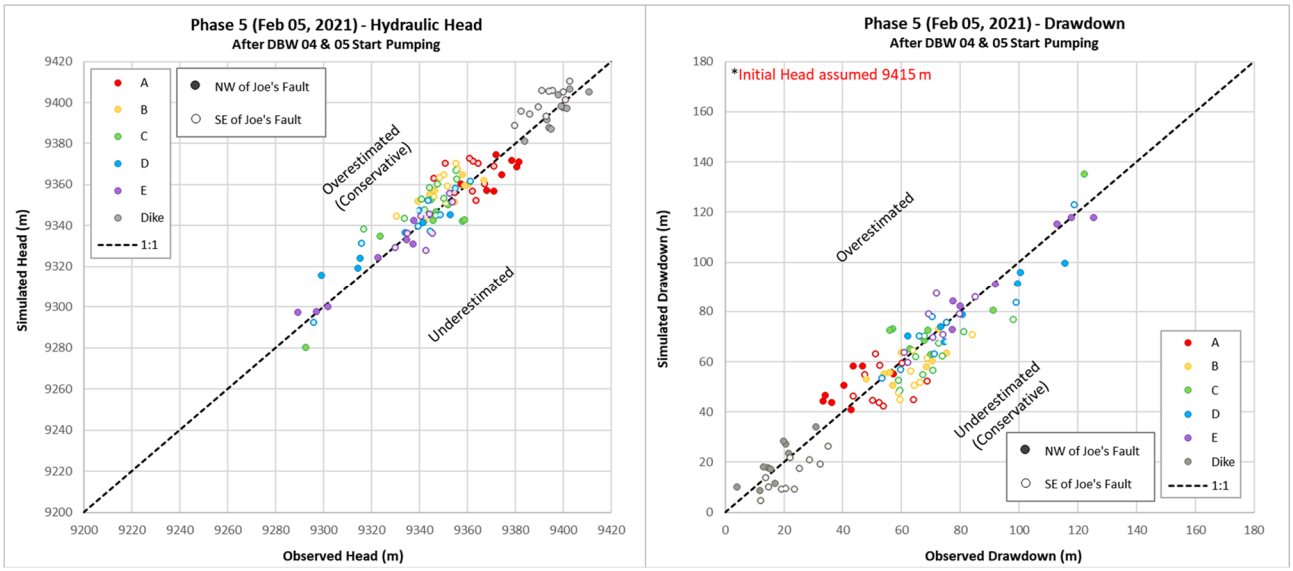


(a) (b)

**Figure 8 (a) Example plot of measured versus predicted hydraulic head and (b) measured versus predicted drawdown – calibration stage 5**

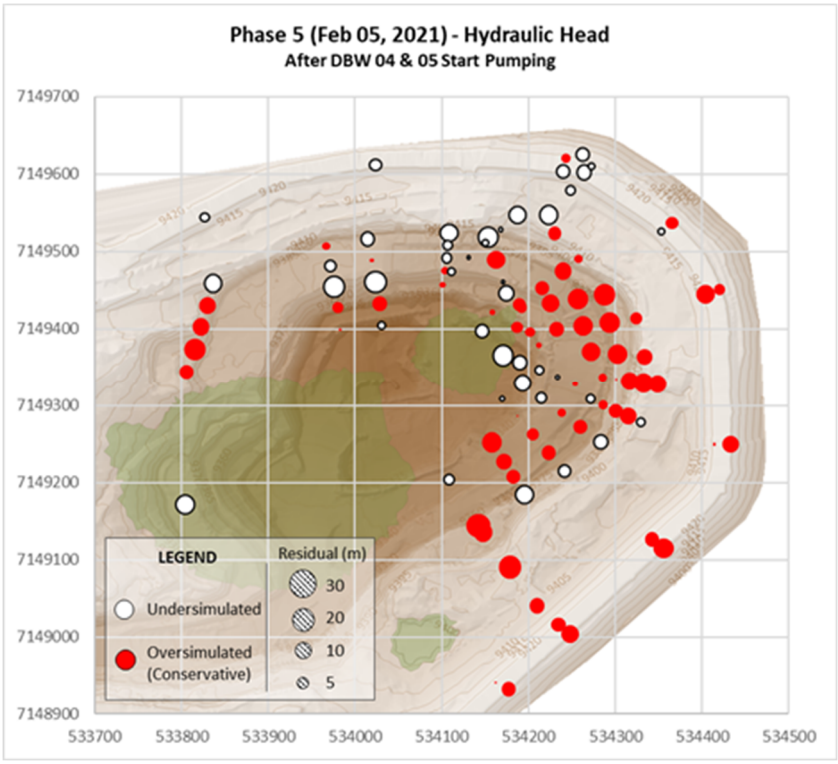


**Figure 9 Example plot of hydraulic head residuals – calibration stage 5. Under-simulated indicates the predicted hydraulic head was lower than measured, whereas over-simulated indicates the predicted hydraulic head was higher than measured**

## 5.1 Estimation of well efficiency

Simulation of future pumping wells in a groundwater model is often done by assigning specified head boundaries, with the assigned hydraulic head set equal to the target water level in the pumping well. This approach inherently assumes a 100% efficient well, which can result in an overestimate of sustainable

pumping rates and magnitude of drawdown in the surrounding bedrock, particularly in a fractured bedrock environment like Diavik.

To evaluate this potential formation inefficiency in the A21 wells, step-drawdown tests were conducted by Diavik Diamond Mines Inc (DDMI) and analysed as part of this assessment. Results of the well efficiency were then considered in the assigned boundary conditions, as described in Section 5.2. The step-drawdown tests were conducted in A21-DP-01 (well 1) and A21-DP-08 (well 5), and consisted of pumping the well at three incremental pumping rates and measuring the response (drawdown) in hydraulic head within the well. Each pumping step was maintained for at least one hour before increasing to the next higher pumping rate.

Collected step test data was evaluated based on equations by Jacob (1946) and Cooper & Jacob (1946), and utilising methodology outlined in Bierschenk (1964) and Driscoll (1986), and included the following steps:

- The specific capacity ($Q/d_{measured}$) for each step was estimated based on the measured pumping rate (Q) and the observed drawdown (s) (Figure 10) at the end of the test (Tables 1 and 2).
- The inverse of the measured specific capacity (also referred to as specific drawdown) was plotted versus the pumping rate, and a linear relationship was fitted to these data (Figure 11) to estimate the turbulent head loss constant (C) and the laminar head loss constant (B). Constants C and B are the slope of the line and intercept of the line with the y-axis, respectively. These data, in combination with the step pumping rates, were used to estimate the percentage of the total head loss that is attributed to laminar flow (Lp) according to the equation Lp = BQ/(BQ + CQ2) * 100.
- The theoretical transmissivity (T) of the well was estimated in AQTESOLV using the Theis (1935) solution for a step-drawdown test and the turbulent well loss parameter (C) from the previous point (Figure 11).
- The theoretical specific capacity of the well was estimated based on the empirical equation by Cooper & Jacob (1946), using the equation ($Q/s_{theoretical} = T/1.04$).
- The well efficiency was then estimated as the ratio of the measured specific capacity to the theoretical specific capacity. Note that for the well installations at A21, which are within fractured bedrock, the turbulent well loss is not attributed to well construction but rather primarily to formation losses associated with pumping in a fractured bedrock environment.

**Table 1 A21-DP-01 (well 1) step test results**

| Step | Pumping rate (Q; $m^3$/day) | Drawdown (s; m) | Measured specific capacity ($Q/S_{measured}$; $m^3$/day/m) | Lp (%) | Transmissivity (T; $m^3$/day) | Theoretical specific capacity ($Q/S_{theoretical}$; ($m^3$/day/m) | Estimated well efficiency (%) |
|---|---|---|---|---|---|---|---|
| 1 | 82 | 8 | 10.3 | 29 | 48 | 46 | 22 |
| 2 | 149 | 26 | 5.7 | 18 | 48 | 46 | 12 |
| 3 | 276 | 76 | 3.6 | 11 | 48 | 46 | 8 |

$m^3$/day = cubic metres per day; m = metres; % = per cent

**Table 2 A21-DP-08 (well 5) step test results**

| Step | Pumping rate (Q; $m^3$/day) | Drawdown (s; m) | Measured specific capacity ($Q/S_{measured}$; $m^3$/day/m) | Lp (%) | Transmissivity (T; $m^3$/day) | Theoretical specific capacity ($Q/S_{theoretical}$; ($m^3$/day/m) | Estimated well efficiency (%) |
|---|---|---|---|---|---|---|---|
| 1 | 76 | 11.3 | 6.7 | 17 | 26 | 25 | 27 |
| 2 | 91 | 16 | 5.7 | 15 | 26 | 25 | 23 |
| 3 | 259 | 116.6 | 2.2 | 6 | 26 | 25 | 9 |

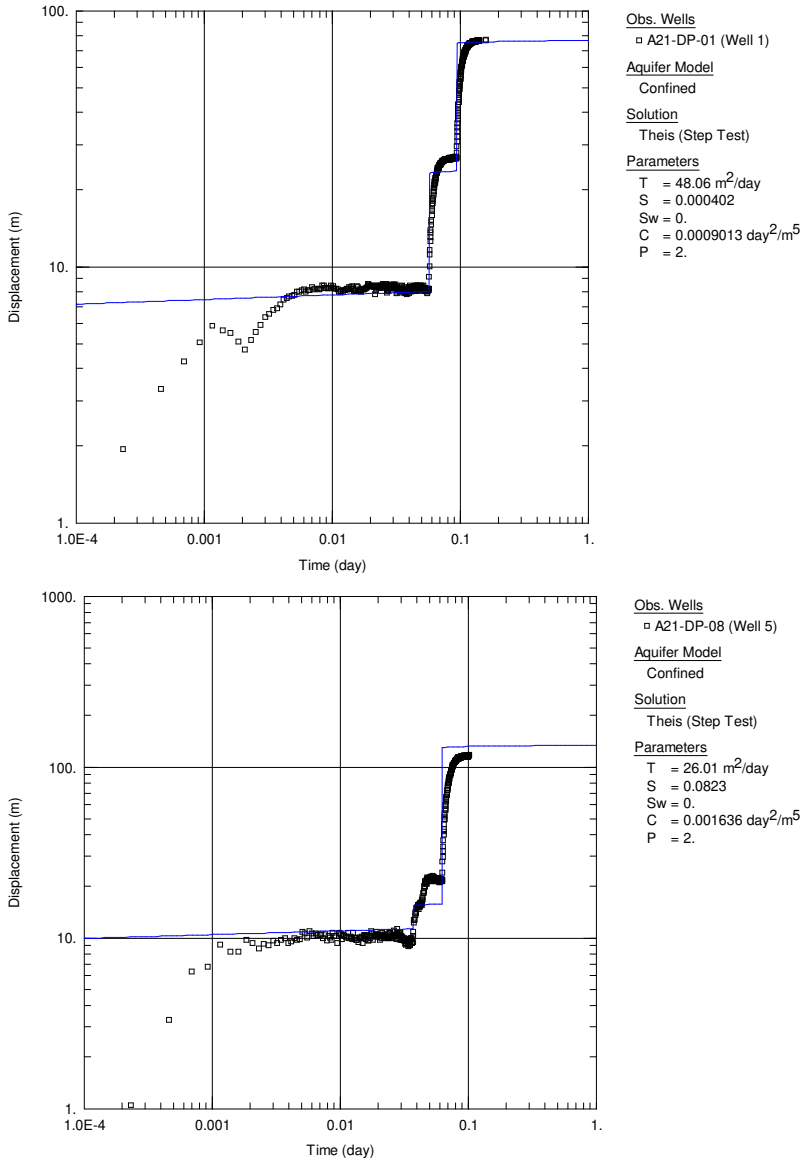


**Figure 10 Pumping test data – wells 1 and 5**

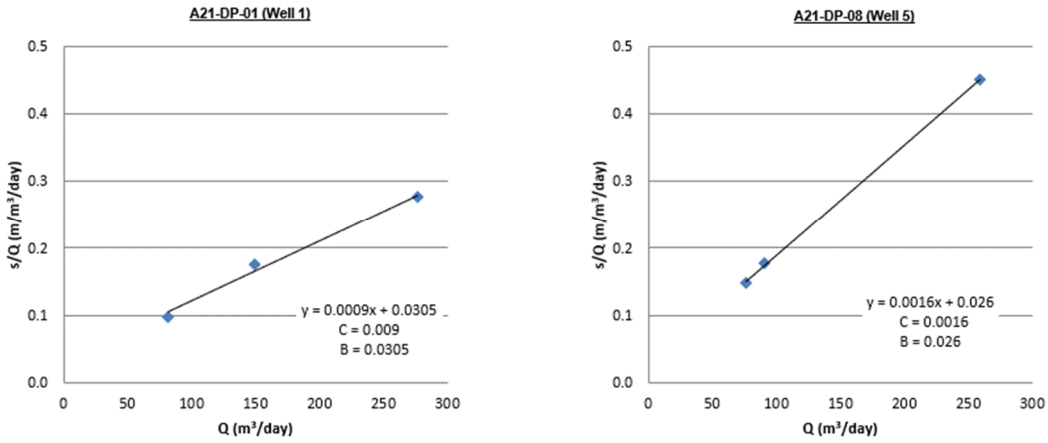


**Figure 11 Step test analysis estimation of laminar and turbulent flow constants**

## 5.2 Incorporation of well efficiency in the numerical model

For calibration periods in the numerical model, where the pumping rate of the depressurisation wells were known, the pumping wells were represented in the model using specified fluxes assigned as a multi-layer well boundary within FEFLOW. During calibration, the assigned flux was the measured pumping rate in the wells.

For predictive simulations, where new wells may be installed or the pumping rates were unknown, a sequenced set of simulations was completed to estimate what the pumping rate of the wells would be, considering the estimated well efficiency of the two-step tested wells. This sequence consisted of:

- A steady-state model run was completed using specified head boundaries to represent the pumping wells, with the pit at its ultimate extent and the assigned hydraulic head set to 20 m above the base of the well. The predicted flow from these specified head boundaries represents the expected pumping rate from the simulated wells, assuming no formation well loss (100% efficient well).
- The predicted flows from the above specified head boundaries were then multiplied by the well efficiency estimated from the step test analysis (8 to 9% at the third stage of pumping). This adjusted flow rate, which accounts for expected formation well loss, was then used in the transient predictive runs for predicting pore pressures over the life of mine with active depressurisation and results in a more realistic estimate of hydraulic head drawdown in the bedrock near the well. This approach assumes formation loss at each of the wells will be similar to that at the two wells tested by DDMI.

The above approach allowed for a more realistic estimate of effectiveness of future depressurisation wells in bedrock environments. This in turn allows for more realistic estimation of well spacing and anticipation of capital costs for their installation. For northern environments where material typically is mobilised on ice roads with limited time windows, estimation of material requirements in advance is critical as unanticipated material requirements often must be transported as air freight.

# 6 Observational mining and manual pore pressure corrections

During mining, pore pressures in the piezometer network were tracked and compared to predicted values from the groundwater model. In late 2022, near the end of the open pit mine life, DDMI indicated that measured monthly pore pressures in the piezometer network were tracking higher than predicted by the groundwater model in the southeast wall of the pit, predominantly at depth in this area. The differences between measured and predicted pore pressures in the southeast wall at depth were thought to indicate

that the Deep Blue zone at depth may not be as wide as previously interpreted from limited drilling data, resulting in predictions of hydraulic heads that were lower than measured values (i.e. the drawdown in this region of the model was overpredicted). As this observation is not conservative for slope stability, a review of the pit stability and pore pressures in this area was undertaken.

As the open pit was near the end of life, insufficient time existed to revise the groundwater model or conduct supplemental drilling to confirm the lateral extents of the Deep Blue zone. As part of an observational mining strategy, stability analysis was conducted on approximately a monthly basis to assess the FoS of critical 2D stability sections considering the observed higher pore pressures. Stability analyses considered month-end topography and month-end measured pore pressures from VWPs. Measured pore pressures from the VWPs were used to manually adjust pore pressure inputs from the groundwater model, as outlined in the following points (and conceptualised in Figures 12 and 13 for a key section in the southeast pit wall):

- Residual pore pressures were calculated for each VWP sensor near the 2D stability section. The residual pore pressure represents the difference between measured and predicted pore pressures (red values in Figure 12).
- Manual adjustments were then made to the predicted pore pressures from the groundwater model along the 2D slope stability cross-sections using the calculated residuals and assuming the pit face is at atmospheric pressure. An example of the before and after pore pressure correction is presented on Figure 13.

The FoS targets for the overall pit slope and for potential failure surfaces breaking back to the downstream toe of the water-retention dyke were achieved for all analyses conducted, and the pit walls exhibited adequate slope stability during the assessed time period. If existing geotechnical and hydrogeological models developed for the A21 pit continue to be used in pit and underground studies, further characterisation of the Deep Blue zone will be considered.

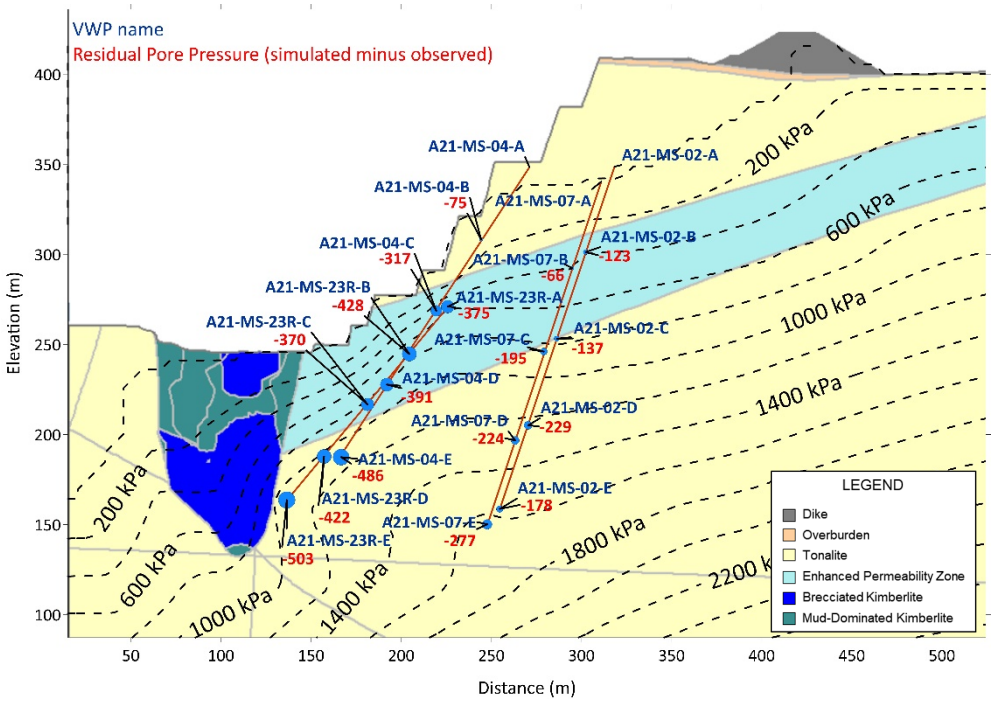


**Figure 12 Pore pressure residuals along the southeast stability section**

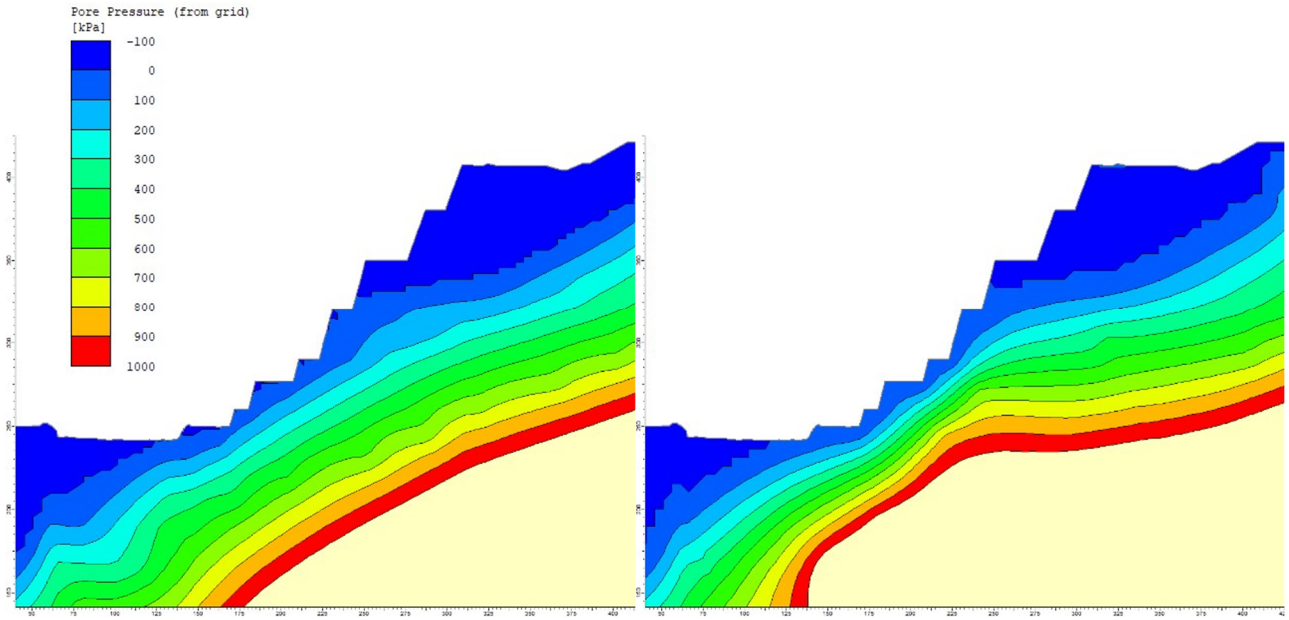


(a) (b)

**Figure 13 (a) Predicted pore pressures and (b) manually adjusted pore pressures along the southeast section**

# 7 Summary and conclusions

Design of the pit depressurisation systems and prediction of pore pressures behind the pit slopes in complex bedrock environments are often undertaken using numerical groundwater models. Over the course of the mine life at A21, multiple revisions of the hydrogeological model were made as supplemental data was collected for this purpose. Key steps in this revision that supported effective estimation of pore pressures in the pit walls included:

- Effective review of the data collected during the installation of the first phase of dewatering wells. Review of airlifting data from development of the wells and observed head changes in piezometers during testing of the dewatering wells led to the identification of a significant enhanced permeability feature in the southeast wall affecting pore pressures.
- Adoption of a practical approach to model calibration given the inherent uncertainty in modelling fractured bedrock environments. Model calibration did not strive to achieve the more typical industry standard of 10% NRMSE but instead sought an overall slight tendency to overpredict hydraulic heads, which is conservative for slope stability analysis. Areas of significant underprediction of hydraulic heads were communicated to the geotechnical teams for increased consideration in the uncertainty analysis of the slope stability analysis.
- Observed well efficiency of installed wells was considered in the method of simulation for future wells. This approach allowed for more realistic estimation of the effectiveness of each well to lower pore pressures, which supported effective planning for the mine site.
- Verification of model predictions through pore pressure monitoring at the VWPs identified that, late in the mine life, the observed hydraulic head was higher than predicted by the groundwater model at depth in the southeast portion of the site (i.e. there was an overprediction of drawdown). Stability analyses conducted using manually corrected pore pressures confirmed that the FoS of critical slopes met DAC near the end stage of mining when insufficient time existed to complete a formal update of the groundwater model.

## Acknowledgement

The authors acknowledge Rio Tinto, Diavik Diamond Mines (2012) Inc. and their employees for their support, collaboration and permission to share the results of this work.

## References

Bierschenk, WH 1964, *Determining Well Efficiency by Multiple Step-Drawdown Tests*, International Association of Scientific Hydrology, Berkeley.

Cooper, HH & Jacob CE 1946, 'A generalized graphical method for evaluation formation constants and summarizing well field history', *American Geophysical Union Transaction*, vol. 27, no. 4, pp. 526–534.

Driscoll, FG 1986, *Groundwater and Wells Second Edition*, US Filter/Johnston Screens, St Paul.

Jacob, CE 1946, 'Drawdown test to determine effective radius of artesian well', *American Society of Civil Engineers Transaction*, vol. 112, pp. 1047–1070.

Theis, CV 1935, 'The relation between the lowering of the piezometric surface and the rate and duration of discharge of a well using groundwater storage', *American Geophysical Union Transaction*, vol. 16, pp. 519–524.